

Assessing Polyglutamine Conformation in the Nucleating Event by Molecular Dynamics Simulations

Markus S. Miettinen,^{*,†,||} Volker Knecht,[‡] Luca Monticelli,^{§,⊥,||} and Zoya Ignatova^{*,†}

[†]Institute of Biochemistry and Biology, University of Potsdam, Karl-Liebknecht-Str. 24-25, 14476 Potsdam, Germany

[‡]Department of Theory and Bio-Systems, Max Planck Institute of Colloids and Interfaces, Am Mühlenberg 1, 14476 Potsdam, Germany

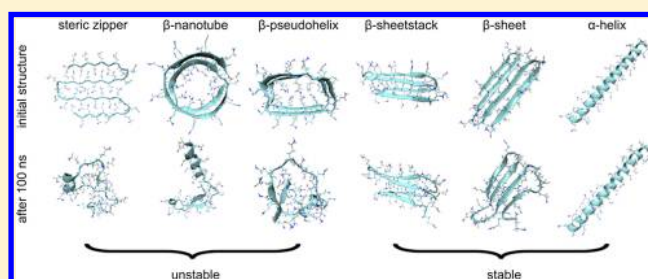
[§]INSERM, UMR-S665, Paris, F-75015, France

[⊥]UMR-S665, Université Paris Diderot, Sorbonne Paris Cité, Paris, F-75013, France

^{||}INTS, F-75015 Paris, France

Supporting Information

ABSTRACT: Polyglutamine (polyQ) diseases comprise a group of dominantly inherited pathology caused by an expansion of an unstable polyQ stretch which is presumed to form β -sheets. Similar to other amyloidopathies, polyQ amyloidogenesis occurs via a nucleated polymerization mechanism, and proceeds through energetically unfavorable nucleus whose existence and structure are difficult to detect. Here, we use atomistic molecular dynamics simulations in explicit solvent to assess the conformation of the polyQ stretch in the nucleus that initiates polyQ fibrillization. Comparison of the kinetic stability of various structures of polyQ peptide with a Q-length in the pathological range (Q_{40}) revealed that steric zipper or nanotube-like structures (β -nanotube or β -pseudo-helix) are not kinetically stable enough to serve as a template to initiate polyQ fibrillization as opposed to β -hairpin-based (β -sheet and β -sheetstack) or α -helical conformations. The selection of different structures of the polyQ stretch in the aggregation-initiating event may provide an alternative explanation for polyQ aggregate polymorphism.



■ INTRODUCTION

Polyglutamine (polyQ) diseases comprise a group of at least nine dominantly inherited neurodegenerative disorders with late onset, including Huntington's disease and several spinocerebellar ataxias.¹ The pathology of these disorders is linked to a common unstable homopolymeric CAG-encoded polyQ-repeat which has an inherent ability to aggregate when the length of this stretch expands over a critical threshold.^{1,2} The disease threshold differs for each disease and for huntingtin, the protein which is implicated in Huntington's disease, the threshold is approximately 35 consecutive glutamines.¹ The impact of the fibrillar, end-stage aggregates on the disease pathology, however, is still controversial. The proposed roles for the fibrillar aggregates range from being central for the pathology and toxicity to being benign or even neuroprotective.^{3,4} Current models propose a direct link between the abundance of earlier small aggregates and cytotoxicity and disease pathology.⁵ Moreover, each of the polyQ diseases displays a distinct cytotoxic pattern and is associated with a unique topography of brain regions, which could be modulated by the sequences flanking the polyQ stretch,^{6,7} cell-type specific mutations and processing^{8,9} or alterations in the localization pattern when the polyQ stretch expands.¹⁰

Aggregation of disease-related polyQ proteins is a multistep process and different sequences from the whole protein participate in each step of the aggregation process.^{11–16} The initial step is polyQ-independent and expansion of polyQ over the pathological threshold triggers the nucleated conformational conversion of oligomers into fibrils^{15,17–19} with the polyQ sequence involved in the core of the fibrillar aggregates.^{13,14,16} Importantly, even proteins with polyQ lengths in the nonpathological range can also form inclusions in the cell, whose associations are mostly driven by the sequences flanking the polyQ stretch.^{13,20} Thus, the aggregation of polyQ proteins is consistent with the nucleated conformational conversion of oligomers into fibrils, which has been also suggested for other amyloidogenic proteins.^{18,21,22}

The dominant role of the polyQ sequence and its intrinsic propensity to trigger aggregation has been demonstrated by the insertion of an expanded polyQ stretch in a nonpathogenic protein causing a progressive neurological phenotype in both *Drosophila* and mice.^{23,24} This raised the question as to whether polyQ peptides can be used to understand the

Received: May 24, 2012

Revised: July 2, 2012

Published: July 6, 2012

biophysics underlying the polyQ-driven fibrillization. PolyQ peptides with pathological repeat lengths aggregate in a nucleated polymerization mechanism.^{25–27} In the thermodynamic model for nucleated polymerization, the nucleation event is extremely rare and the nucleus is defined as the species on the aggregation path that has the highest free energy; the overall efficiency of nucleation depends on the concentration of the nucleus and the rate of elongation.^{28,29} The mechanism by which polyQ peptides aggregate is suggested to be similar to the aggregation of the polyQ proteins^{30,31} where oligomeric nonamyloidogenic species are initially formed in a polyQ-dependent manner. Using a thorough protocol to remove any preformed aggregates that may act as seeds and therefore alter the aggregation pathway, another study has shown that polyQ peptides with a nonpathological Q-length aggregate through a tetrameric (Q_n , $n \leq 23$) or dimeric ($24 < n < 26$) nucleus, whereas the aggregation of peptides with a pathological Q-length is initiated via a monomeric nucleus²⁷ which is an alternatively folded monomer in equilibrium with the native-state monomer.²⁶ The conformational dynamics within the monomer defines the thermodynamic barrier to the monomeric nucleus²⁵ and the growth of the aggregate in the elongation phase depends on the productive reaction of this alternatively folded monomer with the monomer in solution.²⁹

Expanded polyQ sequences in solution are intrinsically disordered,^{32,33} although their conformation does not resemble a canonical random coil and is rather collapsed.³⁴ The aggregation-initiating monomer could contain either β -sheet elements in common with the structure of polyQ fibrils³⁵ or alternating β -strand/ β -turn structure as indicated by substitutions within the polyQ peptides of β -turn-enhancing D-proline-glycine pairs which accelerate aggregation.^{36,37} The β -sheet structure is also consistent with a polyQ structure suggested by the analysis of X-ray data³⁸ of polyQ fibrils.³⁹ However, the same X-ray data were also interpreted as water-filled nanotubes³⁸ and a qualitatively similar structure was accessible in a recent coarse-grained molecular dynamics simulation of dimers.⁴⁰ Another computational study suggests a dry core β -pseudohelix as the monomer conformation in the polyQ fibrils.⁴¹ Alternatively, the polyQ peptides may adopt an α -helical conformation bundled in coiled-coil structures which regulate aggregation, insolubility, and activity of polyQ-containing proteins with their cellular interaction partners.⁴² As the nucleus represents a very small fraction of the bulk monomer, it is inherently difficult to experimentally access the structure of these short-lived and rare species that initiate aggregation. Thus, the conformation of the polyQ stretch in the nucleus remains unknown.

In an effort to address this question, we sought to systematically analyze the kinetic stability of various structures of a polyQ peptide with a length in the pathological range (Q_{40}) using atomistic molecular dynamics simulations. As the nucleus is a transient species and the elongation phase depends on the productive interactions with the native monomer or other alternatively folded species,²⁹ we reasoned that the kinetic stability of the conformer should provide a time window which is long enough to allow interaction between the nucleus with another native or alternatively folded polyQ monomer. Thus, we assessed the kinetic stability of polyQ monomers with various conformations within 100 ns. Even though the simulation time might be shorter than the time needed to establish peptide–peptide interactions, our rationale was that if a structure is unstable over tens of nanoseconds, it is unlikely to

be the conformation that the polyQ stretch adopts in the aggregation-initiating event. We tested six different structures previously suggested in the literature using two different atomistic force fields and explicit solvation, spanning a total simulation time of 12 μ s. Using realistic models and several repeats (20×100 ns), we ranked the α -helical and β -sheet structured polyQ stretches as the most feasible candidates to nucleate the fibrillization of the polyQ peptides. These data provide a solid reference to reconcile independent observations for different structures of the polyQ stretch in the aggregation-initiating event. Approaches to target this conformation may prove to be viable therapeutic strategies for the family of polyQ neuropathologies.

METHODS

Computational Simulations. Two identical sets of simulations were performed using the united-atom GROMOS 43a1⁴³ or with the all-atom CHARMM27^{44,45} force fields. The GROMOS 43a1 simulations were performed using GROMACS version 4.0.7,⁴⁶ with simple point charge (SPC) water,⁴⁷ heavy hydrogens,⁴⁸ reaction field electrostatics ($\epsilon_{\text{rf}} = 54$), and a 4 fs time step. The neighbor lists ($r = 1.4$ nm) were updated after every step, and the van der Waals and Coulomb interactions cut off at 1.4 nm. The CHARMM27 simulations were performed using GROMACS version 4.5.3,⁴⁶ TIP4P water,⁴⁹ particle mesh Ewald^{50,51} electrostatics (4th-order interpolation, 1.3 nm real-space cutoff, relative error in the direct and reciprocal space 10^{-5} , size-optimized fast Fourier transform parameters), and a 2 fs time step. The neighbor lists ($r = 1.3$ nm) were updated after every 10 steps, and the van der Waals interactions were switched off between 1.0 and 1.2 nm. Each of the 120 simulations had periodic dodecahedron boundary conditions (initial distance between the peptide and the face of the unit cell ≥ 1.2 nm); an isotropically coupled ($\tau = 1.0$ ps) Parrinello–Rahman barostat⁵² controlling the pressure at 1.0 bar; and the velocity rescale thermostat⁵³ separately coupled to the peptide and water ($\tau = 0.1$ ps for GROMOS 43a1 and 1.0 ps for CHARMM27) controlling the temperature (310 K). The covalent bonds were constrained to their equilibrium lengths by the fourth-order single-iteration Parallel Linear Constraint Solver⁵⁴ in the Q_{40} and SETTLE⁵⁵ in the water. All six initial nucleus conformers had intact amino and carboxy termini and were hand-built using PyMol (version 1.2r3pre, Schrödinger, LLC), VMD (www.ks.uiuc.edu/research/vmd), and fragments of structures obtained from previous studies. The structures of the β -nanotube and β -pseudohelix motifs were kindly provided by Dr. David Zanuy,⁴¹ the structure used as a basis for the large loop for the β -sheetstack by Dr. Luciana Esposito,⁵⁶ and the β -hairpin structure used for building the β -sheet and β -sheetstack by Dr. Pawel Sikorski.³⁹ Before we started the simulations, the initial conformers were relaxed through two energy minimizations using the steepest descent algorithm: first without and then with constraints. Water was then added and relaxed while restraining the conformation of the peptide. In CHARMM27 this was done in two stages: 5000 steps of 0.2 fs followed by 50 000 steps of 2 fs. In GROMOS 43a1 the latter was sufficient (25 000 steps of 4 fs). Finally, 10 identical copies of each of the 12 systems were given new uncorrelated particle velocities from the Maxwell–Boltzmann distribution at 310 K.

RESULTS AND DISCUSSION

A Steric Zipper Conformation Was the Most Unstable Conformation for the polyQ Stretch. The steric zipper conformer (Figure 1a) is motivated by the parallel superpleated β -structure model for various amyloid fibrils.⁵⁷ It has a serpentine pleated backbone, with interdigitated side chains. The backbone hydrogen bonds point out from the backbone

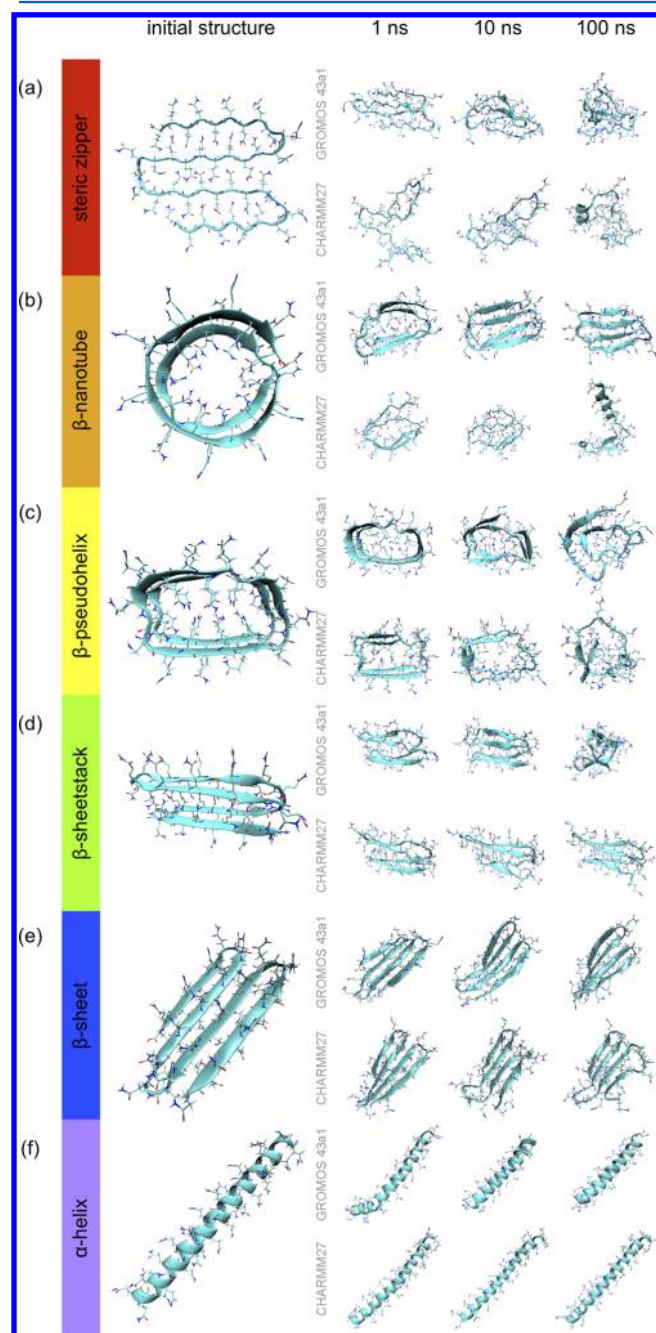


Figure 1. Snapshots of the initial structures (large images) and single continuous trajectories after 1, 10, and 100 ns. The structures are ordered from top to bottom in an increasing order of stability. For each structure, the upper row displays a simulation with the GROMOS 43a1 force field⁴³ and the lower with CHARMM27.^{44,45} In each case a representative trajectory is shown—all the 120 trajectories are available as video in the Supporting Information. Water is omitted for clarity. The snapshots and video were created using VMD;⁷⁶ secondary structures were determined using the STRIDE algorithm.

plane, allowing fibril growth in this direction. Moreover, a recent solid-state NMR study concluded that a steric zipper motif is the building block of polyQ fibrils with 15, 38, and 54 polyglutamines.³⁵ Our simulations with the Q₄₀ peptide proved that the steric zipper conformation for the Q₄₀ monomer was highly unstable. With both force fields, the initial conformation was lost within a nanosecond (Figure 1). The rapid breakage was even more evident from the analysis of the root mean squared deviation (rmsd) from the initial structure (Figure 2),

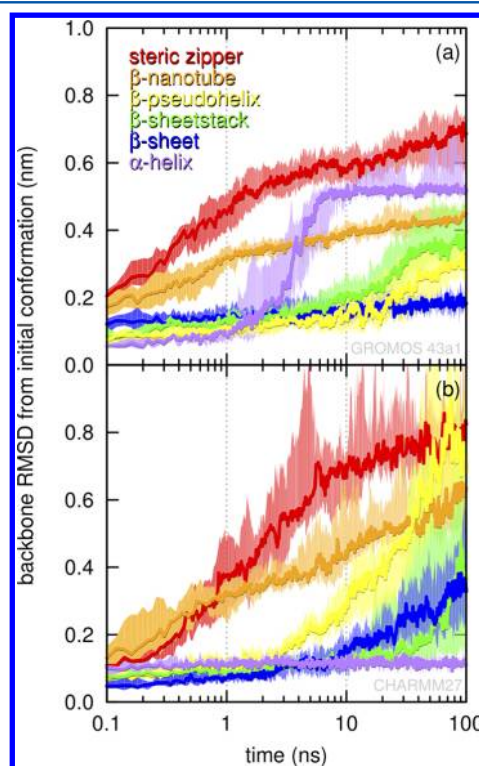


Figure 2. Root mean squared deviation (rmsd) of the backbone atom distances from those of the initial conformer shown as a function of time. Simulations using (a) GROMOS 43a1 and (b) CHARMM27. Median (solid line) and interquartile range (shaded) of 10 replicas are shown. Color coding of conformers is the same as in Figure 1. The rmsds were calculated using the GROMACS 4.5.3 tool `g_rmsdist`.

where with both force fields major changes took place within hundreds of picoseconds. A slight force field specific bias occurred after breaking the conformation, as some β -sheet structure developed with the GROMOS 43a1 force field and some α - and 3_{10} -helices with the CHARMM27 (Figure 3, a and g). Thus, it is highly unlikely that the polyQ stretch takes up the steric zipper conformation in the aggregation nucleating event. The consistent massive breakage on a subnanosecond time scale (Figure 2) suggests that the conformer might not be even a local minimum in the free energy landscape of Q₄₀. The parallel superpleated β -structure proposed for many amyloid proteins is composed of four-residue strands and three-residue turns⁵⁷ and the optimal strand length of 15 residues is suggested for polyQ fibrils.³⁵ One might envision trying to build a structure by varying the length of the strands or the type of the turns, but the rapid total breakage of the steric zipper in our analysis indicates a lack of stabilizing interactions along the strands and suggests that, even with a modification, such conformation of the monomer would be unstable.

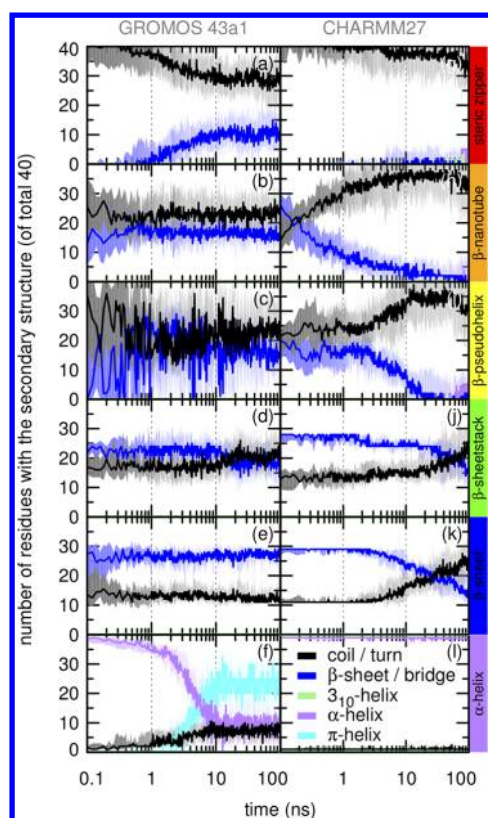


Figure 3. Secondary structure content as a function of time. Results using GROMOS 43a1 (left) and CHARMM27 (right) are compared for each conformer. Median (solid line) and interquartile ranges (shaded) for 10 replicas are shown. The order of the conformers (rows) is the same as in Figure 1. Secondary structures were determined using the STRIDE algorithm.⁷⁶

β -Nanotube and β -Pseudohelix Are Unlikely To Represent the Conformation of the polyQ Stretch in the Aggregation-Initiating Event. The water-filled β -nanotube (Figure 1b) was originally proposed from the analysis of the X-ray spectra of polyQ fibrils.³⁸ This conformation was also recently observed in coarse-grained replica-exchange molecular dynamics simulations of dimers,⁴⁰ yet our analyses revealed that Q_{40} peptide was unstable in the β -nanotube conformation (Figure 1b and video in the Supporting Information). With both force fields, the water molecules rapidly left the cavity of the β -nanotube, and major structural changes occurred within the first nanosecond (Figure 2). Using GROMOS 43a1, planar β -sheet structures developed within 10 ns (Figure 1b and video in the Supporting Information). Interestingly, this occurred without significant alterations to the secondary structure content (Figure 3b). With CHARMM27, β -sheet structure was almost completely lost within 10 ns and some helical motifs appeared during tens of nanoseconds (Figure 3h).

The β -nanotube appears to be marginally more stable than the steric zipper, raising the question of whether the polyQ stretch in such a conformation could be a likely candidate for an aggregation-nucleating conformer. As opposed to our results, earlier computational studies using heavily simplified models found that polyQ peptides with pathological Q-length spontaneously form stable β -nanotubes.^{58,59} However, simulations using more detailed models, including atomistic protein description and explicit water, are in agreement with our

findings. Preformed β -nanotubes of polyQ peptides with similar Q-lengths as used here are stable for up to a few nanoseconds,^{60,61} but are clearly destabilized within 10 ns and water is expelled from the nanotube interior.^{41,62} However, these findings suggest that a dry-core β -pseudohelix (Figure 1c) is a more likely conformer for the monomer that nucleates polyQ fibrillization. Simulations of a polyQ peptide with 84 glutamines in implicit solvent reveal that the structure is stable for up to 30 ns.⁴¹ In our simulations, all of the 20 Q_{40} β -pseudohelix replicas retained the initial structure for 10 ns, and eight of the 10 GROMOS 43a1 replicas even kept the structure until 100 ns (Figure 1c and video in the Supporting Information). Conversely, only one of the 10 CHARMM27 replicas was stable until 100 ns. This difference in the force field predictions was highlighted by the rmsd and the secondary structure content, with only minor changes being observed with GROMOS 43a1 (Figures 2a and 3c), whereas dramatic alterations were detected with CHARMM27 (Figures 2b and 3i).

Therefore, our results do not reveal conclusive evidence to support extended stability of the β -pseudohelix conformation. Instead, we would not expect the conformer to be stable beyond tens of nanoseconds. This time scale mirrors the findings from simulations with other β -helices in explicit solvent, showing that the β -nanotube is unstable after 20 ns, independent of its shape (e.g., circular structure with 40 glutamines or triangular with 36 glutamines).⁶³ Thus, we conclude that the β -pseudohelix is unlikely to be the conformation of the polyQ stretch in the aggregation-initiating event.

PolyQ Stretch in a β -Sheetstack Conformation Is Moderately Stable.

The β -sheetstack (Figure 1d) conformer has been recently proposed as a model for aggregation critical nuclei that are tetrameric for Q_n , $n \leq 23$, dimeric for $24 < n < 26$, or monomeric for $n \geq 26$.²⁷ The structure comprises two β -hairpins linked by a loop and stacked with interdigitated side chains, in a manner similar to the steric zipper. In our simulations, the β -sheetstack was visually more stable than the steric zipper, β -nanotube, or β -pseudohelix conformations (see video in the Supporting Information). With CHARMM27 five out of 10 replicas maintained their original appearance until 100 ns. In four simulations, the two hairpins separated while still maintaining their secondary structure. Only in one of the 10 simulations the secondary structure was lost. A single GROMOS 43a1 replica retained its conformation until 100 ns, while in other replicas visible rearrangements took place after tens of nanoseconds. Importantly, no replica completely lost its original double- β -hairpin structure and eight replicas retained stability for 100 ns. Both force fields showed a low average rmsd until 10 ns, followed by a steady growth over tens of nanoseconds, at which point the repeats started to deviate from the initial β -sheetstack (Figure 2). Accordingly, the secondary structure (Figure 3) only changed after 10 ns.

Typically, the β -sheetstack conformation was stable in our simulation on the 100 ns time scale, and should therefore be considered a possible candidate for the nucleation of polyQ fibrillization. To our knowledge, the stability of a β -sheetstack monomer had not been previously tested, but a somewhat similar conformer of Q_{57} , with four β -strands forming two β -sheets with interdigitated side chains, was stable over 50 ns in earlier all-atom explicit solvent simulations.⁵⁶ The key difference compared to the β -sheetstack is that in this Q_{57} conformer the β -strands were parallel in the β -sheets, leading to an overall

helical topology. Interestingly, for shorter polyQ peptides with pathological lengths (Q_{41}) the authors reported difficulties in constructing monomers with helical topology and interdigitated side chains.⁵⁶ Instead, they had to convert the monomer to a structure similar to the β -pseudohelix presented here.

The β -Sheet Conformation Is Very Stable for the polyQ Stretch. The β -sheet (Figure 1e) conformation is suggested as a good candidate by several studies. Reinterpretation of the X-ray data on polyQ fibrils, which originally were suggested to be water-filled β -nanotubes,³⁸ concluded that β -sheets are the most likely structure of the polyQ in the fibrils.³⁹ Furthermore, a mutational study suggested that the polyQ stretch forms an antiparallel β -sheet with seven glutamines forming the extended strands and four glutamines comprising the loops.³⁷ In addition, β -sheet monomers of thioredoxin–polyQ fusion proteins were found to be cytotoxic and to precede fibrillar assembly.⁶⁴ Compared to the steric zipper, β -nanotube, β -pseudohelix, and β -sheetstack conformations, β -sheet was the most stable conformation. With both force fields the initially flat β -sheet twisted during the first nanosecond (Figure 1e). In GROMOS 43a1 all 10 replicas were stable within the simulation time scale, both in terms of rmsd (Figure 2a) and secondary structure (Figure 3e). Using CHARMM27, seven replicas persisted until 100 ns, whereas three lost stability after tens of nanoseconds (see video in the Supporting Information). Similar to the observations with the β -sheetstack, this was associated with a drift toward a coil-like secondary structure (Figure 3k), and an increase in the rmsd (Figure 2b).

Clearly, the β -sheet is a viable candidate for the conformation of the polyQ stretch that nucleates polyQ fibrillization. Both force fields predict typical β -sheet monomers to be stable beyond 100 ns, which would leave time for establishing intermolecular interactions and elongation. It should be noted, however, that although polyQ monomers with a Q-length ranging from 15 to 47 spontaneously sample β -sheet motifs,^{65–68} individual β -hairpins with 15 or 16 glutamines lose stability in less than 10 ns according to atomistic simulations.^{68,69} Intriguingly, a four-stranded antiparallel β -sheet with 42 glutamines appeared visually stable over a single 10 ns simulation.⁷⁰ Combined with our extensive simulations, these findings suggest that β -structures often occur in polyQ monomers, but do not gain high stability until growing to a minimum of three, or preferably four, strands.

α -Helix Shows Similar Stability to the β -Sheet Conformation for the polyQ Stretch. Our interest in the α -helix conformation (Figure 1f) stems from a recent study which was based on analyses of the interaction partners of polyQ proteins.⁴² Moreover, the conformation of polyQ peptides in vitro with circular dichroism suggests that polyQ peptides form helical coiled coils and assemble into multimers.⁴² This view that monomeric polyQ stretches can obtain α -helical features is supported by observations by simulation^{40,68,71} and experimental^{64,72} studies.

Notably, among all six conformers that were simulated in this study, the α -helix was the most stable with 19 out of 20 replicas retaining helical structure for 100 ns. All CHARMM27 replicas maintained their original conformation without alterations (Figure 1f), as highlighted by the secondary structure (Figure 3l) and rmsd analysis (Figure 2b). In GROMOS 43a1, however, the α -helix thickened and shortened between 1 and 10 ns (Figure 1f), becoming largely π -helical (Figure 3f). We noted that α -to- π -transformations in molecular dynamics simulations are typically viewed as force field artifacts,⁷³ and,

as such, the main information drawn from the GROMOS 43a1 simulations was the general stability of the helical conformation, but not its exact classification.

The observed high kinetic stability of the α -helix conformer qualifies it as a possible candidate for the aggregation-initiating nucleus. A pathogenic expansion of polyQ could generate longer coils that can more easily establish side-to-side interactions, and therefore acquire a stronger polymerization tendency.⁴² We wish to emphasize, however, that the observed high kinetic stability of the α -helix could reflect the common occurrence of α -helical motifs of polyQ stretches with a nonpathological length.⁷²

CONCLUSIONS

Here, we performed systematic analyses to assess the conformation of the polyQ stretch in the nucleus which initiates polyQ-fibrillization using atomistic molecular dynamics simulations in explicit solvent. We determined the kinetic stability of various structural models as possible candidates to nucleate polyQ fibrillization. Comparison of the kinetic stabilities reveals that steric zipper or nanotube-like conformers (β -nanotube or β -pseudohelix) are not kinetically stable enough to nucleate polyQ fibrillization, whereas β -hairpin-based (β -sheet and β -sheetstack) or α -helical conformations could have this potential. In the homogeneous polymerization model,⁷⁴ only two species are relevant and the nucleus serves as a template to initiate fibrillization²⁶ of the ordered β -sheet polyQ fibril. Therefore, in the context of these nucleation–elongation mechanisms initiated by a monomeric nucleus,²⁶ an α -helical conformation might be counterintuitive. However, the rate of elongation of the polyQ peptides is slower than the molecular diffusion,²⁶ implying that ordered template needs to be further deformed or entangled to promote elongation.⁷⁵ Using a heterogeneous model⁷⁵ which allows for incorporating the oligomers observed in the aggregation of polyQ peptides,³⁰ the α -helix is a conceivable structure of the polyQ stretch in the nucleating event. Moreover, the propensity of the α -helical coiled-coil structures to assemble in vitro into multimers⁴² is consistent with the nucleated conformational conversion mechanism.¹⁸ Our data cannot favor a single conformation of the polyQ stretch in the nucleating event. However, given that aggregates with different morphologies are accessible to the polyQ proteins, it is also conceivable that polyQ stretch may exist in a range of alternative conformations undergoing assembly via various aggregation mechanisms.

ASSOCIATED CONTENT

Supporting Information

A video showing the time-evolution of the 120 simulated systems. This material is available free of charge via the Internet at <http://pubs.acs.org>.

AUTHOR INFORMATION

Corresponding Author

*E-mail: markus.miettinen@iki.fi (M.S.M.); ignatova@uni-potsdam.de (Z.I.). Tel.: +49 331 977 5130. Fax: +49 331 977 5128.

Present Address

^{||}Fachbereich Physik, Freie Universität Berlin, 14195 Berlin, Germany.

Author Contributions

M.S.M. performed the simulations and analyzed the data; all authors discussed the results and wrote the manuscript.

Notes

The authors declare no competing financial interest.

ACKNOWLEDGMENTS

The authors thank Drs David Zanuy, Luciana Esposito, and Pawel Sikorski for sharing their molecular structures. We thank Cristiano L. Dias, Praveen Nedumpully Govindan, and Christoph R  thlein for inspiring discussions. M.S.M. acknowledges the support from the Finnish Foundation for Technology Promotion (TES), the HPC-Europa2 visitor project (#228398, supported by the European Commission—Capacities Area—Research Infrastructures), and the European Molecular Biology Organization fellowship (EMBO ALTF 1251-2010). This work was supported by the Deutsche Forschungsgemeinschaft (IG 73/8-1) grant to Z.I.

REFERENCES

- (1) Orr, H. T.; Zoghbi, H. Y. *Annu. Rev. Neurosci.* **2007**, *30*, 575–621.
- (2) Scherzinger, E.; Sittler, A.; Schweiger, K.; Heiser, V.; Lurz, R.; Hasenbank, R.; Bates, G. P.; Lehrach, H.; Wanker, E. E. *Proc. Natl. Acad. Sci. U.S.A.* **1999**, *96*, 4604–4609.
- (3) Arrasate, M.; Mitra, S.; Schweitzer, E. S.; Segal, M. R.; Finkbeiner, S. *Nature* **2004**, *431*, 805–810.
- (4) Kuemmerle, S.; Gutekunst, C. A.; Klein, A. M.; Li, X. J.; Li, S. H.; Beal, M. F.; Hersch, S. M.; Ferrante, R. J. *Ann. Neurol.* **1999**, *46*, 842–849.
- (5) Ross, C. A.; Poirier, M. A. *Nat. Rev. Mol. Cell. Biol.* **2005**, *6*, 891–898.
- (6) Andresen, J. M.; Gayan, J.; Djousse, L.; Roberts, S.; Brocklebank, D.; Cherny, S. S.; Cardon, L. R.; Gusella, J. F.; MacDonald, M. E.; Myers, R. H.; et al. *Ann. Hum. Genet.* **2007**, *71*, 295–301.
- (7) Duennwald, M. L.; Jagadish, S.; Muchowski, P. J.; Lindquist, S. *Proc. Natl. Acad. Sci. U.S.A.* **2006**, *103*, 11045–11050.
- (8) Kennedy, L.; Evans, E.; Chen, C. M.; Craven, L.; Detloff, P. J.; Ennis, M.; Shelbourne, P. F. *Hum. Mol. Genet.* **2003**, *12*, 3359–3367.
- (9) Mende-Mueller, L. M.; Toneff, T.; Hwang, S. R.; Chesselet, M. F.; Hook, V. Y. *J. Neurosci.* **2001**, *21*, 1830–1837.
- (10) Toneff, T.; Mende-Mueller, L.; Wu, Y.; Hwang, S. R.; Bunday, R.; Thompson, L. M.; Chesselet, M. F.; Hook, V. J. *Neurochem.* **2002**, *82*, 84–92.
- (11) de Chiara, C.; Menon, R. P.; Dal Piaz, F.; Calder, L.; Pastore, A. *J. Mol. Biol.* **2005**, *354*, 883–893.
- (12) Ellisdon, A. M.; Thomas, B.; Bottomley, S. P. *J. Biol. Chem.* **2006**, *281*, 16888–16896.
- (13) Hinz, J.; Lehnhardt, L.; Zakrzewski, S.; Zhang, G.; Ignatova, Z. *J. Biol. Chem.* **2012**, *287*, 2068–2078.
- (14) Ignatova, Z.; Thakur, A. K.; Wetzel, R.; Gierasch, L. M. *J. Biol. Chem.* **2007**, *282*, 36736–36743.
- (15) Tam, S.; Spiess, C.; Auyeung, W.; Joachimiak, L.; Chen, B.; Poirier, M. A.; Frydman, J. *Nat. Struct. Mol. Biol.* **2009**, *16*, 1279–1285.
- (16) Thakur, A. K.; Jayaraman, M.; Mishra, R.; Thakur, M.; Chellgren, V. M.; Byeon, I. J.; Anjum, D. H.; Kodali, R.; Creamer, T. P.; Conway, J. F.; et al. *Nat. Struct. Mol. Biol.* **2009**, *16*, 380–389.
- (17) Jayaraman, M.; Kodali, R.; Sahoo, B.; Thakur, A. K.; Mayasundari, A.; Mishra, R.; Peterson, C. B.; Wetzel, R. *J. Mol. Biol.* **2012**, *415*, 881–899.
- (18) Lee, J.; Culyba, E. K.; Powers, E. T.; Kelly, J. W. *Nat. Chem. Biol.* **2011**, *7*, 602–609.
- (19) Liebman, S. W.; Meredith, S. C. *Nat. Chem. Biol.* **2010**, *6*, 7–8.
- (20) Stenoien, D. L.; Mielke, M.; Mancini, M. A. *Nat. Cell Biol.* **2002**, *4*, 806–810.
- (21) Abedini, A.; Raleigh, D. P. *Protein. Eng. Des. Sel.* **2009**, *22*, 453–459.
- (22) Williamson, J. A.; Loria, J. P.; Miranker, A. D. *J. Mol. Biol.* **2009**, *393*, 383–396.
- (23) Marsh, J. L.; Walker, H.; Theisen, H.; Zhu, Y. Z.; Fielder, T.; Purcell, J.; Thompson, L. M. *Hum. Mol. Genet.* **2000**, *9*, 13–25.
- (24) Ordway, J. M.; Tallaksen-Greene, S.; Gutekunst, C. A.; Bernstein, E. M.; Cearley, J. A.; Wiener, H. W.; Dure, L. S. t.; Lindsey, R.; Hersch, S. M.; Joep, R. S.; et al. *Cell* **1997**, *91*, 753–763.
- (25) Bhattacharyya, A. M.; Thakur, A. K.; Wetzel, R. *Proc. Natl. Acad. Sci. U.S.A.* **2005**, *102*, 15400–15405.
- (26) Chen, S.; Ferrone, F. A.; Wetzel, R. *Proc. Natl. Acad. Sci. U.S.A.* **2002**, *99*, 11884–11889.
- (27) Kar, K.; Jayaraman, M.; Sahoo, B.; Kodali, R.; Wetzel, R. *Nat. Struct. Mol. Biol.* **2011**, *18*, 328–336.
- (28) Slepko, N.; Bhattacharyya, A. M.; Jackson, G. R.; Steffan, J. S.; Marsh, J. L.; Thompson, L. M.; Wetzel, R. *Proc. Natl. Acad. Sci. U.S.A.* **2006**, *103*, 14367–14372.
- (29) Wetzel, R. *Nat. Chem. Biol.* **2006**, *2*, 297–298.
- (30) Lee, C. C.; Walters, R. H.; Murphy, R. M. *Biochemistry* **2007**, *46*, 12810–12820.
- (31) Legleiter, J.; Mitchell, E.; Lotz, G. P.; Sapp, E.; Ng, C.; DiFiglia, M.; Thompson, L. M.; Muchowski, P. J. *J. Biol. Chem.* **2010**, *285*, 14777–14790.
- (32) Altschuler, E. L.; Hud, N. V.; Mazrimas, J. A.; Rupp, B. *FEBS Lett.* **2000**, *472*, 166–168.
- (33) Altschuler, E. L.; Hud, N. V.; Mazrimas, J. A.; Rupp, B. *J. Pept. Res.* **1997**, *50*, 73–75.
- (34) Crick, S. L.; Jayaraman, M.; Frieden, C.; Wetzel, R.; Pappu, R. V. *Proc. Natl. Acad. Sci. U.S.A.* **2006**, *103*, 16764–16769.
- (35) Schneider, R.; Schumacher, M. C.; Mueller, H.; Nand, D.; Klaukien, V.; Heise, H.; Riedel, D.; Wolf, G.; Behrmann, E.; Raunser, S.; et al. *J. Mol. Biol.* **2011**, *412*, 121–136.
- (36) Poirier, M. A.; Jiang, H.; Ross, C. A. *Hum. Mol. Genet.* **2005**, *14*, 765–774.
- (37) Thakur, A. K.; Wetzel, R. *Proc. Natl. Acad. Sci. U.S.A.* **2002**, *99*, 17014–17019.
- (38) Perutz, M. F.; Finch, J. T.; Berriman, J.; Lesk, A. *Proc. Natl. Acad. Sci. U.S.A.* **2002**, *99*, 5591–5595.
- (39) Sikorski, P.; Atkins, E. *Biomacromolecules* **2005**, *6*, 425–432.
- (40) Laghaei, R.; Mousseau, N. *J. Chem. Phys.* **2010**, *132*, 165102.
- (41) Zanuy, D.; Gunasekaran, K.; Lesk, A. M.; Nussinov, R. *J. Mol. Biol.* **2006**, *358*, 330–345.
- (42) Fiumara, F.; Fioriti, L.; Kandel, E. R.; Hendrickson, W. A. *Cell* **2010**, *143*, 1121–1135.
- (43) Schuler, L. D.; Daura, X.; van Gunsteren, W. F. *J. Comput. Chem.* **2001**, *22*, 1205–1218.
- (44) Bjelkmar, P.; Larsson, P.; Cuendet, M. A.; Hess, B.; Lindahl, E. *J. Chem. Theory Comput.* **2010**, *6*, 459–466.
- (45) Mackerell, A. D., Jr.; Feig, M.; Brooks, C. L., 3rd. *J. Comput. Chem.* **2004**, *25*, 1400–1415.
- (46) Hess, B.; Kutzner, C.; van der Spoel, D.; Lindahl, E. *J. Chem. Theory Comput.* **2008**, *4*, 435–447.
- (47) Berendsen, H. J. C.; Postma, J. P. M.; van Gunsteren, W. F.; Hermans, J. In *Intermolecular Forces*; Pullman, B., Ed.; Reidel: Dordrecht, The Netherlands, 1981; pp 331–342.
- (48) Feenstra, K. A.; Hess, B.; Berendsen, H. J. C. *J. Comput. Chem.* **1999**, *20*, 786–798.
- (49) Jorgensen, W. L.; Chandrasekhar, J.; Madura, J. D.; Impey, R. W.; Klein, M. L. *J. Chem. Phys.* **1983**, *79*, 926–935.
- (50) Darden, T.; York, D.; Pedersen, L. *J. Chem. Phys.* **1993**, *98*, 10089–10092.
- (51) Essman, U.; Perela, L.; Berkowitz, M. L.; T. Darden, H. L.; Pedersen, L. G. *J. Chem. Phys.* **1995**, *103*, 8577–8592.
- (52) Parrinello, M.; Rahman, A. *J. Appl. Phys.* **1981**, *52*, 7182–7190.
- (53) Bussi, G.; Donadio, D.; Parrinello, M. *J. Chem. Phys.* **2007**, *126*, 014101.
- (54) Hess, B. *J. Chem. Theory Comput.* **2008**, *4*, 116–122.
- (55) Miyamoto, S.; Kollman, P. A. *J. Comput. Chem.* **1992**, *13*, 952–962.

- (56) Esposito, L.; Paladino, A.; Pedone, C.; Vitagliano, L. *Biophys. J.* **2008**, *94*, 4031–4040.
- (57) Kajava, A. V.; Baxa, U.; Wickner, R. B.; Steven, A. C. *Proc. Natl. Acad. Sci. U.S.A.* **2004**, *101*, 7885–7890.
- (58) Khare, S. D.; Ding, F.; Gwanmesia, K. N.; Dokholyan, N. V. *PLoS Comput. Biol.* **2005**, *1*, 230–235.
- (59) Marchut, A. J.; Hall, C. K. *Proteins* **2007**, *66*, 96–109.
- (60) Ogawa, H.; Nakano, M.; Watanabe, H.; Starikov, E. B.; Rothstein, S. M.; Tanaka, S. *Comput. Biol. Chem.* **2008**, *32*, 102–110.
- (61) Merlino, A.; Esposito, L.; Vitagliano, L. *Proteins: Struct., Funct., Bioinf.* **2006**, *63*, 918–927.
- (62) Stork, M.; Giese, A.; Kretzschmar, H. A.; Tavan, P. *Biophys. J.* **2005**, *88*, 2442–2451.
- (63) Rossetti, G.; Magistrato, A.; Pastore, A.; Persichetti, F.; Carloni, P. *J. Phys. Chem. B* **2008**, *112*, 16843–16850.
- (64) Nagai, Y.; Inui, T.; Popiel, H. A.; Fujikake, N.; Hasegawa, K.; Urade, Y.; Goto, Y.; Naiki, H.; Toda, T. *Nat. Struct. Mol. Biol.* **2007**, *14*, 332–340.
- (65) Lakhani, V. V.; Ding, F.; Dokholyan, N. V. *PLoS Comput. Biol.* **2010**, *6*, e1000772.
- (66) Vitalis, A.; Lyle, N.; Pappu, R. V. *Biophys. J.* **2009**, *97*, 303–311.
- (67) Wang, X.; Vitalis, A.; Wyczalkowski, M. A.; Pappu, R. V. *Proteins* **2006**, *63*, 297–311.
- (68) Nakano, M.; Watanabe, H.; Rothstein, S. M.; Tanaka, S. *J. Phys. Chem. B* **2010**, *114*, 7056–7061.
- (69) Armen, R. S.; Bernard, B. M.; Day, R.; Alonso, D. O. V.; Daggett, V. *Proc. Natl. Acad. Sci. U.S.A.* **2005**, *102*, 13433–13438.
- (70) Zhang, Q. C.; Yeh, T.-l.; Leyva, A.; Frank, L. G.; Miller, J.; Kim, Y. E.; Langen, R.; Finkbeiner, S.; Amzel, M. L.; Ross, C. A.; et al. *J. Biol. Chem.* **2011**, *286*, 8188–8196.
- (71) Wang, Y.; Voth, G. A. *J. Phys. Chem. B* **2010**, *114*, 8735–8743.
- (72) Kim, M. W.; Chelliah, Y.; Kim, S. W.; Otwinowski, Z.; Bezprozvanny, I. *Structure* **2009**, *17*, 1205–1212.
- (73) Feig, M.; Mackerell, A. D., Jr.; Brooks, C. L., 3rd. *J. Phys. Chem.* **2003**, *107*, 2831–2836.
- (74) Ferrone, F. *Methods Enzymol.* **1999**, *309*, 256–274.
- (75) Vitalis, A.; Pappu, R. V. *Biophys. Chem.* **2011**, *159*, 14–23.
- (76) Frishman, D.; Argos, P. *Proteins* **1995**, *23*, 566–579.